

# Metal–Metal Distances, Electron Counts, and Superconducting $T_C$ 's in $AM_2B_2C$

Claudia Felser

Institut für Anorganische Chemie und Analytische Chemie, Johannes Gutenberg-Universität, Duesbergweg 10-14, D55099, Mainz, Germany

Received September 7, 2000; in revised form March 22, 2001; accepted April 9, 2001; published online July 3, 2001

We present first principles band structure calculations on representative boron carbides belonging to the class of superconducting compounds with the general formula  $AM_2B_2C$  with  $A = \text{Lu, La, or Th}$  and  $M = \text{Ni or Pd}$ . The compounds are analyzed within the framework of the so-called van Hove scenario, where superconductivity is linked to certain kinds of instabilities in the band structure. We attempt to determine why the addition of the extra electron on replacing the rare earth with Th does not make a significant difference to the superconducting properties, and why the compound  $\text{LaNi}_2\text{B}_2\text{C}$  is not superconducting. © 2001 Academic Press

**Key Words:** superconductor; borocarbides; structure and bonding; electronic structure.

## 1. INTRODUCTION

The finding of superconductivity with transition temperatures up to 23 K in boron carbides and boron nitrides (1–4) crystallizing in a stuffed variant of the  $\text{ThCr}_2\text{Si}_2$  structure type has raised the question of whether these materials constitute a new class of high-temperature superconductors.

The electronic band structures of these compounds and especially of  $\text{LuNi}_2\text{B}_2\text{C}$  have been investigated by different methods at different levels by several groups (5–20). In this contribution, rather than focusing on a single compound, we compare aspects of the electronic structures of representative compounds from this interesting new class of materials. The compounds discussed are  $ANi_2B_2C$  with  $A = \text{Lu, La, or Th}$  and the compound  $\text{ThPd}_2\text{B}_2\text{C}$ . At the end of this exercise, we expect to have determined what effect the change in size of the  $A$  ion (going from Lu to La) and the change in the electron count (going from the rare earths to Th) might have on the electronic structure and perhaps on the superconducting transition temperature ( $T_C$ ). Among other things, we demonstrate that Th replacement cannot be treated within a simple rigid-band framework.

Within the Bardeen–Cooper–Schrieffer (BCS) theory the transition temperatures are proportional to the density of states at the Fermi energy  $N(E_F)$  provided  $\omega_D$ , the

characteristic electron phonon frequency, does not change significantly for the compounds compared. This corresponds to the empirical rule of Matthias—for a valence electron concentration (VEC, the number of valence electrons per atom) of 4.7, the highest  $T_C$ 's for certain alloys and for the A15 type compounds can be achieved. Just for this VEC, these systems have a peak in their densities of state at  $E_F$ . From this point of view we expect superconductivity in isoelectronic  $\text{LaNi}_2\text{B}_2\text{C}$  and no superconductivity in the Th compounds. Going by this rule alone, it is difficult to understand why  $\text{ThPd}_2\text{B}_2\text{C}$  has nearly the same  $T_C$  as  $\text{LuNi}_2\text{B}_2\text{C}$ . Table 1 compiles some structural and electronic data on some of the compounds examined here, along with their superconducting  $T_C$ 's.

A few groups (6, 19, 21, 22) have focused on a special band in the electronic structures of these compounds. This band crosses  $E_F$  and displays saddle point behavior at the  $X$  point in the vicinity of  $E_F$ . Such a saddle point in the band structure leads to a peak in the density of states often referred to as a van Hove singularity (23) in the case of low-dimensional systems. The van Hove scenario is an attempt to reconcile superconducting transport properties within the BCS theory and was developed to explain the enhanced  $T_C$  of the intermetallic A15 superconductors (24). More recently, approaching the problem of the cuprate high- $T_C$  superconductors from the metallic side, the van Hove scenario has been used to explain the unusually high  $T_C$ 's (25, 26). This is a theme we will follow in the present article, examining the electronic structures of some of the boron carbides with an emphasis on electronic instabilities including van Hove singularities in the vicinity of the Fermi energy.

## 2. STRUCTURES AND CALCULATION PROCEDURE

All boron carbides discussed here,  $AM_2B_2C$  ( $A = \text{Lu, La, and Th}$ ;  $M = \text{Ni, Pd}$ ), adopt a variation of the  $\text{ThCr}_2\text{Si}_2$  structure type (Fig. 1) crystallizing in the  $I4/mmm$  space group. The difference is the carbon atom which stuffs the  $A_4$  squares. For the calculations we have taken the experimentally determined lattice constants (5, 27, 28). For



**TABLE 1**  
**Relation of Superconducting Transition Temperatures to the Electronic and Crystal Structure in  $LnM_2B_2C$**

Compound	$N(E_F)^a$	$M-M$ (Å)	$T_C$ (K)	Ref.
$LuNi_2B_2C$	4.2	2.45	16	(1)
$ThPd_2B_2C$	3.8	2.72	15	(34)
$ThNi_2B_2C$	4.2	2.60	6	(35)
$LaNi_2B_2C$	2.6	2.69	—	(5)

<sup>a</sup>Number of states per formula unit.

$ThPd_2B_2C$ , the values from a single-phase Rietveld refinement were used (29). The B  $z$  parameters, if they were not available, were calculated within the assumption of a meaningful B–C distance. The experimental geometry used for the Th compounds was as follows: Th at the position  $2a$   $(0, 0, 0)$ , Pd(Ni) at the position  $4d$   $(\frac{1}{2}, 0, \frac{1}{4})$ , and B at  $4e$   $(0, 0, z)$ , with  $z = 0.361$  for  $ThPd_2B_2C$  and  $z = 0.356$  for  $ThNi_2B_2C$ . The additional carbon in these compounds occupies  $2b$   $(0, 0, \frac{1}{2})$ .

The structures are mainly characterized by layers of edge-shared  $MX_4$  tetrahedra parallel to the  $ab$  plane and separated by planes of  $A$ . Within the  $MX_4$  tetrahedra the transition metal  $M$ – $M$  distances are very short, being 2.45 Å in  $LuNi_2B_2C$ , the shortest Ni–Ni distance in any compound with the  $ThCr_2Si_2$  type structure, and slightly shorter than in the metal (2.50 Å). We therefore expect strong metal–metal bonding in  $LuNi_2B_2C$ . The same situation is found in  $ThNi_2B_2C$  which has a slightly larger Ni–Ni distance (2.60 Å). In the Pd compound the metal–metal distance (2.72 Å) is also rather short (cf. 2.751 Å in the metal). The boron carbides seem to be three-dimensional from the point of view of the structure with a B–C–B unit associated with a strong bonding interaction linking the layers.

Self-consistent, first principles calculations within the local density approximation (LDA) (30) of the electronic structures of  $LuNi_2B_2C$ ,  $ThNi_2B_2C$ ,  $ThPd_2B_2C$ , and  $LaNi_2B_2C$  were performed using the LMTO method in the atomic sphere approximation (ASA). A detailed description of the LMTO-ASA method and its application to the electronic structure of compounds has been given elsewhere (31, 32). The scalar relativistic Kohn–Sham–Schrödinger equations were solved taking all relativistic effects into account except for the spin–orbit coupling.  $k$ -space integrations used the tetrahedron method to calculate the electronic structure. More than 1000 irreducible  $k$ -points were used within the Brillouin zone (BZ). The BZ is as described in Ref. (33), where the special symmetry points are labelled in accordance with the standard notation corresponding to  $\Gamma$   $(0, 0, 0)$ ,  $X$   $(\frac{1}{2}, \frac{1}{2}, 0)$ ,  $Z$   $(0, 0, \frac{1}{2})$  in the same Brillouin zone and  $Z'$   $(1, 0, 0)$  in the next Brillouin zone. The Brillouin has the shape of a faceted box which is flattened in the  $z$ -direction.

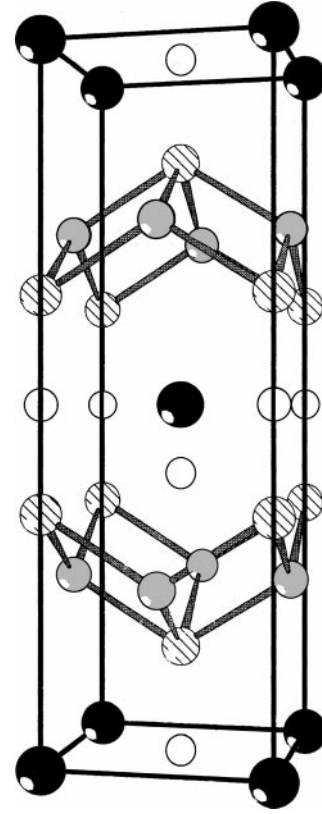


**FIG. 1.** Crystal structure of  $LuNi_2B_2C$ . Black circles correspond to  $Ln$ , gray circles to Ni or Pd, white circles to carbon, and striped circles to boron.

The basis set consisted of  $s$ ,  $p$ ,  $d$ , and  $f$  orbitals for Th,  $s$ ,  $d$ , and  $f$  orbitals for Lu and La,  $s$ ,  $p$ , and  $d$  orbitals for Ni, and  $s$  and  $p$  orbitals for B and C. The Lu and La  $p$  and B and C  $d$  orbitals were handled by a special down-folding procedure (34). The positions and radii of the empty spheres were calculated using an automatic procedure developed by Krier *et al.* (34). Within the so-called fatband representation (35), the orbital character of each band can be easily demonstrated by decorating specific bands with a width that is proportional to the sum of the weights of the corresponding orthonormal orbitals. A pure band state, i.e., a 100% fatband, is given a width that is 2.5% of the energy scale.

### 3. RESULTS AND DISCUSSION

#### 3.1. Density of States

To answer the question of whether the boron carbide superconductors follow the simple relation between the  $T_C$  and  $N(E_F)$  expected of the BCS superconductors, we compare in Fig. 2 the total density of states (DOS) of (a)  $LuNi_2B_2C$ , (b)  $ThPd_2B_2C$ , (c)  $ThNi_2B_2C$ , and (d)  $LaNi_2B_2C$ . As mentioned in the introduction  $LaNi_2B_2C$  is nonsuperconducting, whereas the other compounds are

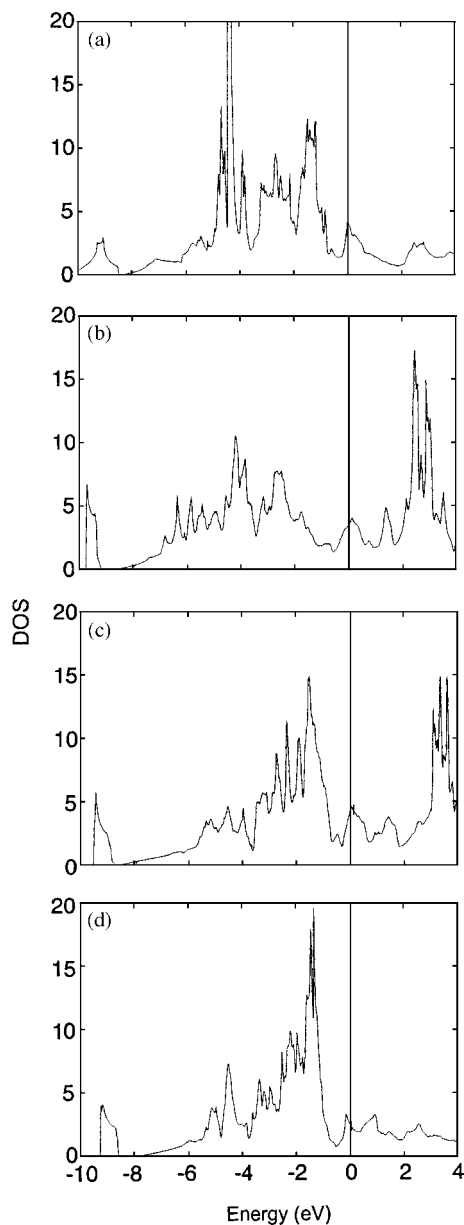


FIG. 2. Total LMTO-ASA density of states for (a)  $\text{LuNi}_2\text{B}_2\text{C}$ , (b)  $\text{ThPd}_2\text{B}_2\text{C}$ , (c)  $\text{ThNi}_2\text{B}_2\text{C}$ , and (d)  $\text{LaNi}_2\text{B}_2\text{C}$ . The vertical lines mark the Fermi energy.

superconductors with different transition temperatures [ $\text{LuNi}_2\text{B}_2\text{C}$ ,  $T_C = 16.5$  K (1);  $\text{ThPd}_2\text{B}_2\text{C}$ ,  $T_C = 15$  K (36);  $\text{ThNi}_2\text{B}_2\text{C}$ ,  $T_C = 6$  K (37)]. Relevant data have been summarized in Table 1. Although the Th compounds have an even number of valence electrons (namely 34), we expect a metal because from the band structure of  $\text{LuNi}_2\text{B}_2\text{C}$  (which has 33 valence electrons) we know that three bands cross  $E_F$ . If we compare the total DOS of the Th compounds, Figs. 2b and 2c with the Lu compound, shown in Fig. 2a, it is surprising that although there is an additional electron in the Th compounds, the total density of states

looks very similar, especially in the vicinity of the Fermi energy.

We also wish to examine the different contributions to the total DOS in order to obtain an overview of the electronic properties of these compounds. We show only the DOS between  $-10$  and  $4$  eV; therefore, the Th  $p$  states ( $-18$  eV) which are included in the calculation as valence electrons are not seen in the DOS. The states with  $a_{1g}$  symmetry, namely the bonding B-C-B  $\sigma$  interactions, are situated between  $-15$  and  $-13$  eV with respect to  $E_F$  in  $\text{LuNi}_2\text{B}_2\text{C}$  and between  $-13$  and  $-12$  eV with respect to  $E_F$  in  $\text{ThPd}_2\text{B}_2\text{C}$  and  $\text{ThNi}_2\text{B}_2\text{C}$ ; these states are not shown in Fig. 2. Boron and carbon  $s$  and  $p$  states contribute to the peak between  $-10$  and  $-8.3$  eV; the corresponding peak is found in  $\text{LuNi}_2\text{B}_2\text{C}$  in the same energy range but is slightly broader. The bottom of the valence band of all compounds is built by B and C  $p_z$  states. Ni or Pd  $d$  states dominate the valence band between  $-8$  eV; and the Fermi energy ( $E_F$ ). The overall band width of the transition metal  $d$  states is higher in the Pd compound than in the Ni compounds. The additional sharp peak in  $\text{LuNi}_2\text{B}_2\text{C}$ ,  $-4.3$  eV with respect to  $E_F$ , is due to the  $4f$  states of Lu. Th  $f$  and La  $f$  states are found around  $3$  eV and  $6$  eV above  $E_F$ .

For three superconducting compounds, namely those with Th- and  $\text{LuNi}_2\text{B}_2\text{C}$ , we find a peaked density of states around  $E_F$ , separated by a pseudogap from the transition metal states. The situation is different for  $\text{LaNi}_2\text{B}_2\text{C}$ , where the Fermi energy falls just in the gap between two small peaks. Even if the highest density of states peak is slightly below  $E_F$  in  $\text{ThNi}_2\text{B}_2\text{C}$  the absolute value at  $E_F$  is the highest (see Table 1). The number of states per unit cell at  $E_F$  is 3.6 in  $\text{ThPd}_2\text{B}_2\text{C}$ , 4.2 for  $\text{ThNi}_2\text{B}_2\text{C}$ , 4.2 for  $\text{LuNi}_2\text{B}_2\text{C}$ , and only 2.6 for  $\text{LaNi}_2\text{B}_2\text{C}$ . In all compounds the contribution of the transition metal is the highest (around 70%). The DOS peak in  $\text{LaNi}_2\text{B}_2\text{C}$  is shifted to lower energies. From the density of states we can conclude that the lowest density of states  $E_F$  is indeed found for nonsuperconducting  $\text{LaNi}_2\text{B}_2\text{C}$ , but  $T_C$  is not related in a linear manner to  $N(E_F)$ . The additional electron in the Th compounds does not shift the Fermi energy, and the electronic structure of these compounds cannot be understood within a simple rigid band model.

### 3.2. Band Structure

In this section we investigate the band structures in some detail because there are still open questions. Can we understand the superconductivity in this compound within the van Hove scenario and does the superconducting transition temperature depend on the position of the van Hove singularity? We also continue to search for the additional electron and which band (and interaction) is influenced by replacement of the rare earth by Th. To answer the first

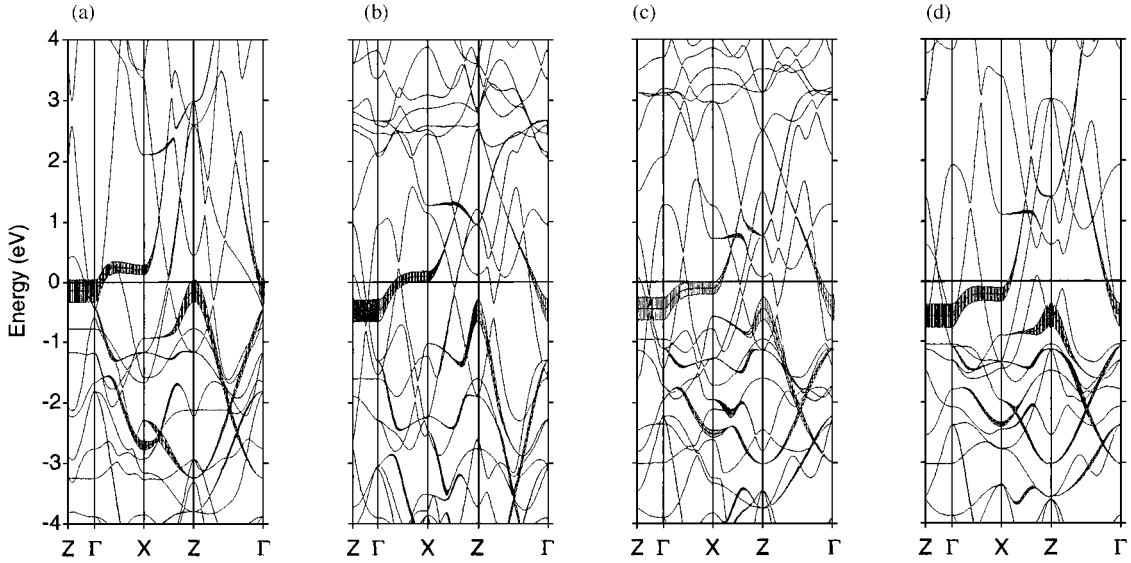


**FIG. 3.** LMT0-ASA band structure for (a)  $\text{LuNi}_2\text{B}_2\text{C}$ , (b)  $\text{ThPd}_2\text{B}_2\text{C}$ , (c)  $\text{ThNi}_2\text{B}_2\text{C}$ , and (d)  $\text{LaNi}_2\text{B}_2\text{C}$  with  $M\text{ }d\bar{d}\sigma^*$  in its fatband representation; 100% eigenvectors contribution corresponds to 0.2 eV.

question we focus on the position of the metal  $dd\sigma^*$  band. This is the band that has the saddle point. Figure 3 shows the metal  $dd\sigma^*$  band of (a)  $\text{LuNi}_2\text{B}_2\text{C}$ , (b)  $\text{ThPd}_2\text{B}_2\text{C}$ , (c)  $\text{ThNi}_2\text{B}_2\text{C}$ , and (d)  $\text{LaNi}_2\text{B}_2\text{C}$ . It seems to be generally true that the  $dd\sigma^*$  band is always in the vicinity of the Fermi energy even when the rare earth metal is replaced by Th. In  $\text{ThPd}_2\text{B}_2\text{C}$  and in  $\text{LuNi}_2\text{B}_2\text{C}$  the saddle point of this antibonding band is found slightly above  $E_F$ , 0.1 and 0.2 eV, respectively, whereas in  $\text{ThNi}_2\text{B}_2\text{C}$  with the lower  $T_C$  the vHS is located around  $-0.2$  eV with respect to  $E_F$ . In the La compound, it is found 0.5 eV below  $E_F$ . Also  $\text{YPd}_2\text{B}_2\text{C}$  and  $\text{YNi}_2\text{B}_2\text{C}$ , compounds which are not subjects of this article, fit nicely into this story. In  $\text{YPd}_2\text{B}_2\text{C}$  the borocarbide with the highest  $T_C$  of 23 K, the  $dd\sigma^*$  band is situated less than 0.05 eV below  $E_F$ . In  $\text{YNi}_2\text{B}_2\text{C}$  with a  $T_C$  similar to that of  $\text{LuNi}_2\text{B}_2\text{C}$  the  $dd\sigma^*$  band is found at the same position, 0.2 eV above  $E_F$ .

The position of the antibonding metal band in  $\text{LaNi}_2\text{B}_2\text{C}$  is nearly the same as in all other  $\text{ThCr}_2\text{Si}_2$  structure type compounds with Ni as the transition metal (21). The cause for this is a larger Ni-Ni distance found in all Ni compounds (for sterical reasons) within the  $\text{ThCr}_2\text{Si}_2$  structure type as well as in  $\text{LaNi}_2\text{B}_2\text{C}$ . The overall band width of the antibonding band in the boron carbides is higher due to the insertion of carbon (22). The peak in the density of states is not precisely correlated with the position of the saddle point. The superconducting properties seem to be correlated with the position of the antibonding metal band. Additional factors, however, seem to be important because although the position of the saddle point is nearer  $E_F$  in  $\text{ThPd}_2\text{B}_2\text{C}$  compared with  $\text{LuNi}_2\text{B}_2\text{C}$ ,  $T_C$  is slightly higher in the latter compound. In both compounds the bands at  $E_F$  show

clearly that this interaction is two-dimensional and no band dispersion along  $\Gamma$  to Z can be observed.

We try to answer the question of which band is half-occupied by the additional electron. As discussed in length elsewhere (21, 22) apart from the *metal-metal* interaction two additional types of interaction, *metal-nonmetal* and *nonmetal-nonmetal*, determine the band structure within the  $\text{ThCr}_2\text{Si}_2$  structure type and the stuffed variants. The  $\sigma$  type interaction of the B-C-B unit in its fatband representation is shown in Figs. 4a and 4b for  $\text{LuNi}_2\text{B}_2\text{C}$  and  $\text{ThPd}_2\text{B}_2\text{C}$ . To the band  $-14$  eV with respect to  $E_F$  at  $\Gamma$ , the  $a_{1g}$  band has only  $s$  eigenvector contribution. All orbitals are in phase. In the case of the second band around  $-9$  eV with respect to  $E_F$  at  $\Gamma$ , there is a node lying in the center of the carbon atom. Boron  $s$  and C  $p_z$  eigenvectors contribute to this band. The third band splits due to the interaction with the  $sd^3$  orbitals of the Ni-B interaction. This interaction is responsible for the contribution of the  $\sigma$  type orbitals to the band which crosses  $E_F$  between  $\Gamma$  and X. From the point of view of the occupation, no significant difference can be observed for  $\text{LuNi}_2\text{B}_2\text{C}$  and  $\text{ThPd}_2\text{B}_2\text{C}$ . We have to recognize, however, that the B-C-B band which crosses  $E_F$  is shifted slightly to higher energy in  $\text{ThPd}_2\text{B}_2\text{C}$ .

This band was discussed in an earlier publication (5) as being important for the superconducting properties. In  $\text{LuNi}_2\text{B}_2\text{C}$  where this band is situated around  $E_F$  touching the vHS band between  $\Gamma$  and X, the position of the band depends strongly on the structural parameters. This influence might be smaller in  $\text{ThPd}_2\text{B}_2\text{C}$ , where the maximum of the band is higher in energy. The bonding interaction between the transition metal and the B will not be discussed in length here, because we will do this elsewhere (22). The

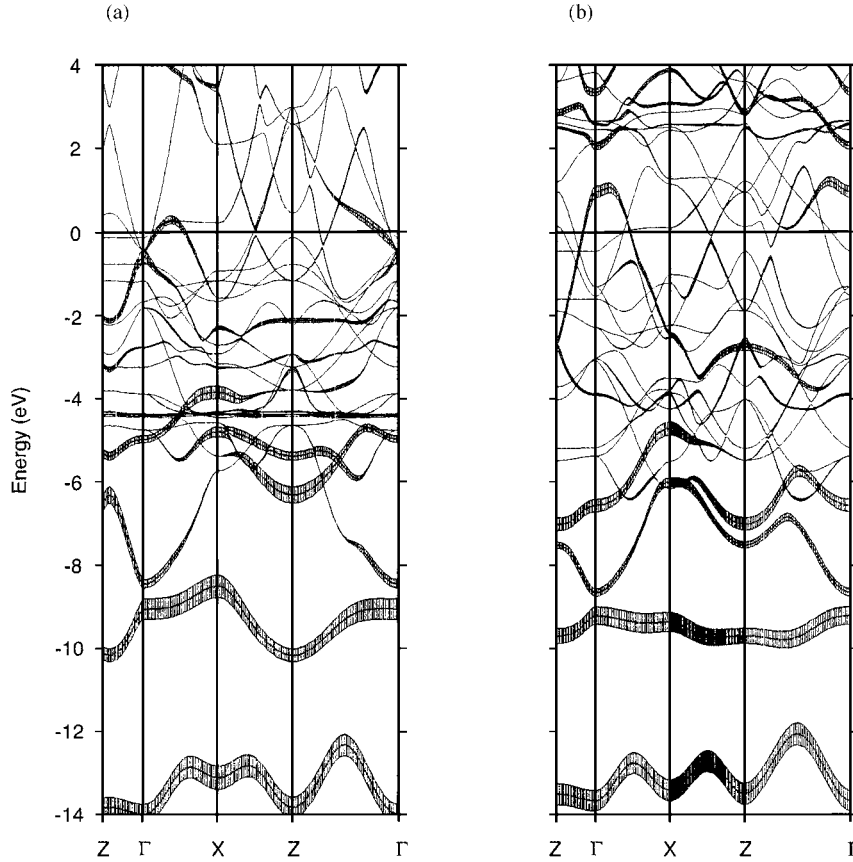


**FIG. 4.** Fatbands of (a)  $\text{LuNi}_2\text{B}_2\text{C}$  and (b)  $\text{ThPd}_2\text{B}_2\text{C}$  projected on the B–C–B  $\sigma$ -type interaction mediated by  $s$  and  $p_z$ ; 100% eigenvectors contribution corresponds to 0.45 eV.

interaction between B and Ni in  $\text{LuNi}_2\text{B}_2\text{C}$  is mediated by the  $sd^3$  orbitals. Ten bands of these  $sd^3$  orbitals are occupied in  $\text{LuNi}_2\text{B}_2\text{C}$  (22). For  $\text{ThPd}_2\text{B}_2\text{C}$  a similar situation is found. The overall band width is higher in  $\text{ThPd}_2\text{B}_2\text{C}$  because of the broader Pd  $d$  orbitals.

Most band structure calculations on the boron carbides point out that the rare earth element in this structure type compounds is not fully ionized. In contrast to the high-temperature superconductors, where the rare earth  $d$  and  $f$  bands are situated above  $E_F$  far away from the saddle point, a significant Lu and Th contribution to the states around  $E_F$  is found. Therefore, we discuss the fatbands of the Lu and Th  $d_{x^2-y^2}$  orbital contribution, shown in Figs. 5a and 5b. The occupation of this band is significantly different in the two compounds. Whereas the Lu  $d_{x^2-y^2}$  bands cause the  $E_F$  to dip only at  $\Gamma$ , building a small electron pocket, the Th  $d_{x^2-y^2}$  band is half-occupied. We conclude, therefore, that the additional electron of the Th compound is found in this band.

### 3.3. Discussion

In summary we can say that the rigid band model is not valid in such a complicated structure as the one adopted by

$\text{ThCr}_2\text{Si}_2$  compounds and its stuffed variants. Going from the rare earth to the Th compound, we expect the additional electron to half-fill a band in  $\text{ThPd}_2\text{B}_2\text{C}$ . This additional electron leads mainly to a change in the position of the Th  $d_{x^2-y^2}$  band. Whereas this three-dimensional band in  $\text{LuNi}_2\text{B}_2\text{C}$  causes the Fermi energy to dip only slightly at the  $\Gamma$  point, the occupation of this band is higher for the Th compound. Additionally, the Fermi energy is slightly raised in  $\text{ThPd}_2\text{B}_2\text{C}$ . Despite the three-dimensionality of the overall band structure, especially due to the not-fully ionized rare earth metal, the superconducting properties in this structure type are seen to be related to the  $dd\sigma^*$  band of the transition metals in the  $MX_4$  layers. These theoretical findings are in agreement with the experimental observation that  $T_C$  is correlated with the nearest neighbor Ni–Ni distance in the planes (38).

In all superconducting compounds this band is situated in the vicinity of the Fermi energy, building a saddle point—a van Hove singularity (vHS) at the X point. We recognize that there are qualitative differences between the high-temperature superconductors and the boron carbides due to the differences in the overall band structures. In the cuprates, where only the band with the saddle point crosses  $E_F$ , a metal-to-insulator transition can take place

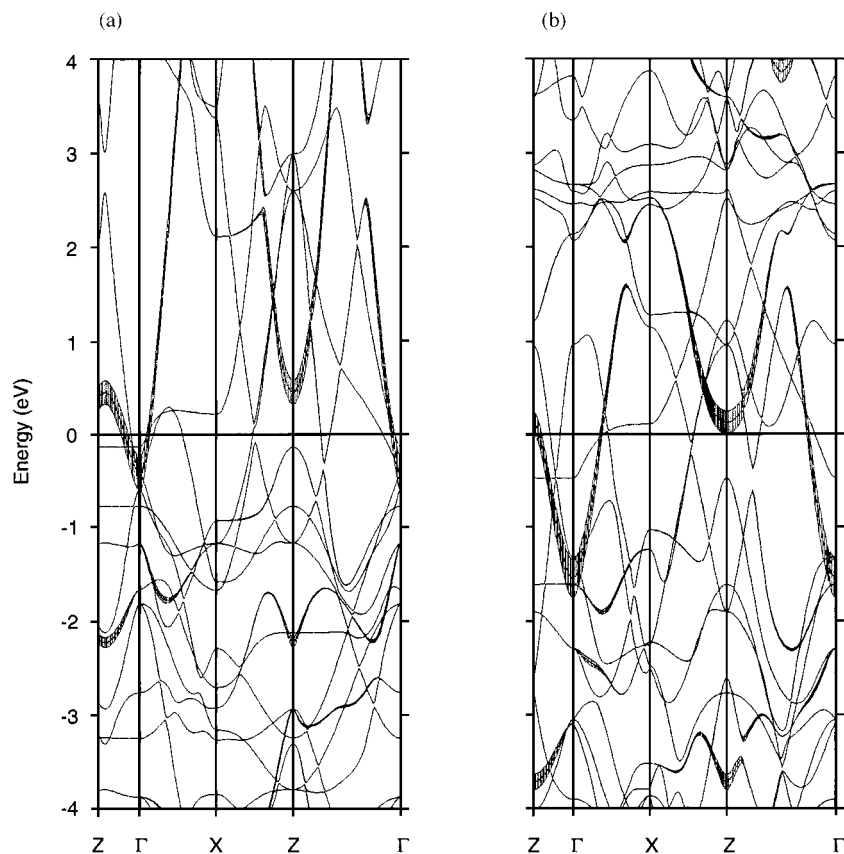


**FIG. 5.** Fatbands of (a)  $\text{LuNi}_2\text{B}_2\text{C}$  and (b)  $\text{ThPd}_2\text{B}_2\text{C}$  with contribution from Lu and Th  $d_{x^2-y^2}$  orbitals; 100% eigenvectors contribution corresponds to 0.2 eV.

depending on the band filling. The three-dimensional rare earth metal band and an additional band which crosses  $E_F$  in the boron carbides avoid such a transition. Therefore, the high-temperature transport properties of the boron carbides are different from those of the cuprates, whereas in the case of the low-temperature behavior similarities like spin fluctuation are observed. We believe that the vHS and the proportionality of  $T_C$  to  $N(E_F)$  in these and other intermetallic compounds are in general two sides of the same coin, because a saddle point also results in a high density of states.

## REFERENCES

1. R. J. Cava, H. W. Zandbergen, B. Batlogg, H. Eisaki, H. Takagi, J. J. Krajewski, W. F. Peck, Jr., and E. M. Gyorgy, *Nature* **372**, 759 (1994).
2. R. J. Cava, H. Takagi, H. W. Zandbergen, J. J. Krajewski, W. F. Peck, Jr., T. Siegrist, B. Batlogg, R. B. van Dover, R. J. Felder, K. Mizukaski, J. O. Lee, H. Eisaki, and S. Uchida, *Nature* **367**, 252 (1994).
3. R. J. Cava, H. Takagi, B. Batlogg, H. W. Zandbergen, J. J. Krajewski, W. F. Peck, R. B. van Dover, R. J. Felder, Jr., T. Siegrist, K. Mizukaski, J. O. Lee, H. Eisaki, and S. Uchida, *Nature* **367**, 146 (1994).
4. R. Nagarajan, C. Mazumdar, Z. Hossain, S. K. Dhar, K. V. Gopalakrishnan, L. C. Gupta, C. Godart, B. D. Padalia, and R. Vijayaraghavan, *Phys. Rev. Lett.* **72**, 274 (1994).
5. L. F. Mattheiss, T. Siegrist, and R. J. Cava, *Solid State Commun.* **91**, 587 (1994).
6. J. I. Lee, T. S. Zhao, I. G. Kim, B. I. Min, and S. J. Youn, *Phys. Rev. B* **50**, 4030 (1994).
7. L. F. Mattheiss, *Phys. Rev. B* **49**, 13279 (1994).
8. W. Pickett and D. J. Singh, *Phys. Rev. Lett.* **72**, 3702 (1994).
9. W. Pickett and D. J. Singh, *Nature* **374**, 682 (1995).
10. W. Pickett and D. J. Singh, *J. Supercond.* **8**, 425 (1995).
11. G. J. Miller, *J. Am. Chem. Soc.* **116**, 6332 (1994).
12. R. Coehorn, *Physica C* **228**, 331 (1994).
13. J.-F. Halet, *Inorg. Chem.* **33**, 4173 (1994).
14. J. K. Burdett and S. Sevov, *Inorg. Chem.* **33**, 3857 (1994).
15. D. J. Singh and W. Pickett, *Phys. Rev. B* **51**, 8668 (1995).
16. H. Kim, C. D. Hwang, and J. Ihm, *Phys. Rev. B* **52**, 4592 (1995).
17. Z. Zeng, D. E. Ellis, D. Guenzburger, and E. M. Baggio-Saitovich, *Phys. Rev. B* **53**, 6613 (1996).
18. P. Ravindran, S. Sankaralingam, and R. Asokamani, *Phys. Rev. B* **52**, 12921 (1995).
19. D. J. Singh, *Phys. Rev. B* **50**, 6486 (1994).
20. D. J. Singh, *Solid State Commun.* **98**, 899 (1996).
21. D. Johrendt, C. Felser, O. Jepsen, O. K. Andersen, A. Mewis, and J. Rouxel, *J. Solid State Chem.* **129**, 254 (1997).
22. C. Felser, O. Jepsen, and O. K. Andersen, to be published.
23. L. van Hove, *Phys. Rev.* **89**, 1189 (1953).
24. J. Labbe and J. Friedel, *J. Phys. (Paris)* **27**, 153 (1966).
25. J. Labbe and J. Bok, *Europhys. Lett.* **3**, 1225 (1987).

26. D. M. Newns, H. R. Krishnamurthy, P. C. Pattnaik, C. C. Tsuei, C. C. Chi, and C. L. Kane, *Physica B* **186**, 801 (1993).
27. T. Siegrist, R. J. Cava, J. Krajewski, and W. F. Peck, Jr., *J. Alloys Compds.* **216**, 135 (1994).
28. R. J. Cava, private communication.
29. P. J. Jiang, Y. Y. Hsu, Y. B. You, K. C. Ku, J. C. Ho, S. H. Lin, Y. D. Yao, and Y. Y. Chen, *Chin. J. Phys.* **34**, 646 (1996).
30. U. von Barth and L. Hedin, *J. Phys. C* **4**, 2064 (1971).
31. O. K. Andersen and O. Jepsen, *Phys. Rev. Lett.* **53**, 2571 (1984); O. K. Andersen, Z. Pawlowska, and O. Jepsen, *Phys. Rev. B* **34**, 5253 (1986).
32. H. L. Skriver, "The LMTO Method." Springer, Berlin, 1984.
33. C. J. Bradley and A. P. Cracknell, "The mathematical theory of symmetry in solid." Clarendon Press, Oxford, 1972.
34. G. Krier, O. Jepsen, and O. K. Andersen, unpublished results.
35. O. Jepsen and O. K. Andersen, *Z. Phys. B* **97**, 35 (1995).
36. H. W. Zandbergen, T. J. Gortenmulder, J. L. Sarrac, J. C. Harrison, M. C. de Andrade, J. Hermann, S. H. Han, Z. Fisk, M. B. Maple, and R. J. Cava, *Physica C* **232**, 328 (1994).
37. Z. Hossain, L. C. Gupta, R. Nagarajan, P. Raj, S. K. Dhar, C. Godart, P. Suryanarayana, S. N. Bagchi, V. G. Date, D. S. C. Purushotham, and R. Vijayaraghavan, *Europhys. Lett.* **28**, 55 (1994).
38. C. C. Lai, M. S. Lin, Y. B. You, and H. C. Ku, *Phys. Rev. B* **51**, 420 (1995).